JOURNAL OF MATERIALS SCIENCE 22 (1987) 2535–2541

Influence of strong grain-boundary pinning by particles upon grain-boundary structure during post-recrystallization anneals

VALERIE RANDLE, BRIAN RALPH*
Institute of Materials, University College, Cardiff, South Glamorgan, UK

A study has been made of grain-boundary geometry as a function of grain-boundary pinning by coherent precipitates in a complex superalloy. About two hundred boundaries have been analysed and the boundary misorientation parameters are interpreted in terms of the coincident site lattice (CSL) theory. The results show a clear correlation between the proportion of CSL boundaries and the amount of pinning interaction between coherent precipitates and boundaries. Where grain-boundary migration has been completely suppressed by strong pinning, almost half the boundaries are of CSL type ($\Sigma \leqslant 49$). These observations are interpreted as an alternative means of minimizing the system's energy when the normal route for energy reduction (grain growth) is blocked. Possible mechanisms for the rotation of grains towards CSL configurations are discussed.

1. Introduction

The formulation of geometrical models which describe the structure of grain-boundaries has progressed to an advanced level (e.g. [1–3]). To a certain extent, the properties of grain-boundaries can be related to their structure. For example, low diffusivities can be correlated with certain coincidence site lattice (CSL) boundaries (e.g. [4, 5]), as can low mobilities (e.g. [6]) and low grain-boundary energies (e.g. [7]). For all of these cases the property does not bear a simple relationship with the density of coincidence sites and much effort is still being directed towards elucidation of the precise parameters which control grain-boundary properties (e.g. [8]). However, it is accepted that certain boundaries are "special" in the sense that their properties differ from "non-special" boundaries and these special boundaries are likely to be described by a fairly low Σ CSL relationship [9]. Therefore, it follows that grain-boundary energy (and other properties) is lower for CSL boundaries as a group than for non-CSL boundaries [10, 11]. Experimental support for theories of boundary structure has been provided almost exclusively by studies of fairly small populations of specially oriented bicrystals, pure metals or simple binary alloys (e.g. [8]). Where precipitates are present in the microstructure – which encompasses most commercially used alloys – there are a number of different ways in which grain boundaries may interact with precipitates. This is particularly true for situations where boundaries are migrating under the influence of a small driving force (e.g. grain growth) and/or the precipitate array is coherent with the matrix (e.g. [12–14]). The effects on grain-boundary misorientation parameters of the presence of a coherent precipitate population has not been previously evaluated. Consequently, the work reported here describes a statistical analysis of boundary geometry in a sample population of grain boundaries in a complex, multiphase alloy. The results are interpreted in terms of the CSL theory (e.g. [15]).

2. Experimental procedure

A nickel-based superalloy, Nimonic PE 16 (Wiggins Alloys), was used for the investigations. Such alloys are precipitation strengthened by the presence of gamma prime, γ', which is based on $Ni_3(Ti, Al)$ and fully coherent with the surrounding matrix. When heat treated for service, the volume fraction of γ' is about 2 to 6% and its diameter 10 nm. Three heat treatments were conducted:

(i) 300 sec at 1100° C followed by a water quench, so that the grain size increased from about 20 to 100 μm and γ' was retained in solution; superlattice reflections were absent from diffraction patterns ("unaged" sample).

(ii) The in-service heat treatment, i.e. water quenched from 1040° C plus 4 h at 700° C so that γ' precipitates were about 10 nm diameter ("aged" sample), and with a mean grain size of about 20 μm.

(iii) Heat treatment as in (ii) plus 1000 h at 830° C so that γ' had coarsened to an average size of 150 nm for intergranular precipitates ("overaged" sample), although the grain size remained pinned at about 20 μm.

Convergent-beam diffraction patterns were obtained from either side of a grain-boundary for a total of about 200 boundaries, representing the three data sets (unaged, aged and overaged). The analysis of grain-boundary misorientation parameters was carried out using a method devised by the present authors which

Present address: Department of Materials Technology, Brunel, University of West London, Uxbridge, UK.

0022–2461/87 $03.00 + .12

is described elsewhere [16]. All transmission electron microscopy was performed with a Philips 400 T microscope.

3. Results

The microstructures after the overageing treatment showed considerable coarsening of the γ' phase but almost the complete absence of grain growth.

An essential prerequisite to the interpretation of the collected geometrical data is the establishment of criteria for the categorization of each boundary. Two classes are identified: the existence of a two-dimensional periodic structure at the boundary defines the CSL classification, and the remaining boundaries are considered to be non-CSL or random. Of course, any boundary may be described in terms of a CSL if the limit on the volume of the CSL unit cell compared with the lattice unit cell, Σ, is infinite. However, it is unclear if any significance in terms of parameters such as diffusivity and energy can be attributed to very long-period boundaries. As there is evidence that small energy cusps exist around certain CSL misorientations whose Σ value is as high as 67 [9] or 83 [7], it is considered reasonable to define boundaries with $\Sigma \leqslant 49$ as CSL and all other boundaries, even when very close to a CSL with $\Sigma > 49$, as non-CSL.

The CSL group are not described as "ordered" here because boundaries which do not conform to CSL limitations may still possess periodicity in one dimension due to the matching of low-index atomic planes across the boundary. This is termed planar matching [17, 18] and clearly such boundaries are also "ordered" although not CSL types. A few boundaries have been observed during the course of this study which clearly show a dislocation substructure yet do not conform to the CSL case. It is presumed that these are planar matching boundaries, although at this stage an analysis to confirm this has not been carried out.

The terms "special" and "non special" as applied to boundaries have also been avoided in describing the present data because as indicated above, they apply to boundary properties rather than boundary geometry. Special low-energy boundaries are not always synonomous with low Σ values. For example, the $\Sigma = 33$ boundary is known to have a lower energy than some lower Σ boundaries [7]. The inclination of the boundary plane also influences grain-boundary energy (e.g. [15, 19]). However, existing experimental results are difficult to interpret unambiguously, and it seems the intuitively reasonable theory that the boundary plane will try to follow the most densely packed directions to the CSL does not always correlate with experimental observation (e.g. [8]). As it is often difficult and time consuming to measure the boundary inclination accurately, especially in the presence of boundary curvature, the results here are confined to axis/angle of misorientation pair data, which specify the misorientation between two adjacent grains.

It remains to decide upon an angular range about an exact CSL configuration that the model might be considered to apply. Deviations from an exact CSL, V, are accommodated by intrinsic grain-boundary dislocations up to a point where dislocation core overlap begins. The magnitude of the three Burgers vectors of the grain-boundary dislocation array vary as $\Sigma^{-1/2}$, $\Sigma^{-1/2}$ and Σ^{-1} [20]. It is therefore reasonable to assume that the maximum angular range for a CSL, V_m, will be proportional to $\Sigma^{-1/2}$ [21], which is the criterion adopted for this work [16]. It is not possible to know V_m exactly since its value will be influenced by the inclination of the boundary plane [22] and also consideration of if the lowest energy situation will result from conservation of a given CSL or minimum Burgers vectors (e.g. [23]).

TABLE I(a) CSL and near CSL boundaries in unaged specimens

Axis/angle for exp. boundary	Axis/angle for CSL boundary	Σ	V_m	V
1 27 0/38.0	100/37.0	5	6.7	1.1
731 688 44/37.0	110/38.9	9	5.0	2.2
988 156 65/21.5	100/22.6	13	4.2	3.0
772 623 44/26.0	100/26.5	19	3.4	2.5
772 627 35/20.7	110/20.1	33	2.6	1.9
676 623 391/62.3	221/61.9	17	3.6	3.2
689 619 378/47.3	221/46.4	29	2.8	2.5
779 469 416/41.8	211/44.4	21	3.3	3.2
972 415 61/33.2	210/35.4	27	2.9	2.9
near CSL				
830 396 393/37.3	211/34.0	35	2.5	2.6
903 326 301/44.5	311/40.5	23	3.1	3.3
986 139 87/30.0	100/28.1	17	3.6	4.0
982 167 92/27.4	100/28.1	17	3.6	4.0

Table I gives details of individual boundaries which were found to be near CSL configurations. The following data are recorded.

Column 1: experimentally determined axis/angle

TABLE I(b) CSL and near CSL boundaries in aged specimens

Axis/angle for exp. boundary	Axis/angle for CSL boundary	Σ	V_m	V
515 546 524/27.2	111/27.2	13	4.2	0.7
591 590 550/57.9	111/60.0	3	8.7	2.2
596 596 538/60.5	111/60.0	3	8.7	2.2
588 530 616/17.0	111/17.9	31	2.7	1.1
820 416 394/46.2	211/44.4	21	3.3	1.5
876 482 29/35.3	210/35.4	27	2.9	1.4
707 704 62/51.1	110/50.5	11	4.5	2.4
786 437 437/33.6	211/34.0	35	2.5	1.5
906 391 225/36.5	311/33.6	33	4.1	2.5
646 581 495/55.7	111/60.0	3	8.7	5.9
717 692 83/51.4	110/50.5	11	4.5	3.2
860 510 18/50.0	210/48.2	15	3.9	2.8
668 567 481/29.4	111/27.8	13	4.1	3.1
692 685 250/39.0	331/37.1	47	2.2	1.7
994 110 13/25.5	100/22.6	13	4.2	3.4
584 477 669/53.5	111/60.0	3	8.7	7.9
887 477 52/51.5	210/48.2	15	3.9	3.5
978 208 105/37.0	100/36.9	5	6.7	6.1
980 190 0/40.0	100/36.9	5	6.7	6.1
984 154 94/40.6	100/36.9	5	6.7	6.3
near CSL				
793 566 225/48.2	321/50.1	39	2.4	2.5
623 671 402/59.8	221/61.9	17	3.6	4.0
759 644 101/51.7	110/50.5	11	4.5	5.1
850 530 70/47.7	210/48.2	15	3.9	4.4
691 605 395/18.3	111/17.9	31	2.7	3.1
857 367 388/30.5	211/34.0	35	2.5	3.3

TABLE I(c) CSL and near CSL boundaries in overaged specimens

Axis/angle for exp. boundary	Axis/angle for CSL boundary	Σ	V_m	V
1 0 0/16.5	100/16.3	25	3.0	0.1
577 587 568/22.0	111/21.8	21	3.3	0.3
719 713 9/38.2	110/38.9	9	5.0	0.7
730 688 35/38.0	110/38.9	9	5.0	1.3
572 607 552/62.5	111/60.0	3	8.7	2.7
910 423 17/35.5	210/35.4	27	2.9	0.9
743 676 0/37.5	110/38.9	9	5.0	1.7
719 695 28/40.5	110/38.9	9	5.0	1.7
605 563 563/14.3	111/15.2	43	2.3	0.8
990 100 0/16.0	100/16.4	25	3.0	1.2
995 078 017/15.5	100/16.4	25	3.0	1.3
650 559 508/60.0	111/60.0	3	8.7	4.7
622 598 505/59.9	111/60.0	3	8.7	4.2
700 655 269/51.6	331/51.7	25	3.0	1.5
614 601 550/54.1	111/60.0	3	8.7	5.1
719 682 70/32.0	110/31.6	27	2.9	1.7
865 501 17/49.5	210/48.2	15	3.9	2.3
807 448 385/52.1	211/52.2	31	2.7	1.9
893 342 284/48.0	311/50.7	15	3.9	2.8
944 476 389/34.3	211/34.0	35	2.5	1.8
980 130 105.22.3	100/22.6	13	4.2	3.1
914 438 35/33.0	210/35.4	27	2.9	2.2
956 305 31/63.5	310/64.6	35	2.5	1.9
963 207 174/48.4	511/50.6	37	2.5	1.9
906 423 113/33.0	210/35.4	27	3.7	2.9
775 570 273/48.9	321/50.1	39	2.4	1.9
957 289 25/45.0	310/43.1	37	2.5	2.0
875 367 342/40.5	311/40.5	23	3.1	2.5
945 330 284/36.0	311/33.6	33	2.6	2.1
748 484 453/47.7	322/49.2	49	2.1	1.7
633 606 482/53.2	111/60.0	3	8.7	7.3
866 522 44/50.0	210/48.2	15	3.9	3.3
975 219 37/37.1	100/36.9	5	6.7	5.8
780 626 6/50.4	110/50.5	11	4.5	4.3
766 629 139/37.0	110/38.9	9	5.0	5.0
707 574 431/18.0	111/17.9	31	2.7	2.7
near CSL				
796 606 39/43.8	110/38.9	9	5.0	5.6
891 446 104/26.0	210/27.9	43	2.3	2.6
848 489 250/48.5	321/50.1	39	2.4	2.8
727 565 392/36.1	111/38.2	7	5.7	6.7
783 616 199/62.0	431/65.0	45	2.2	2.6
629 545 537/44.0	111/43.6	49	2.1	2.5
958 274 80/48.0	331/51.7	25	3.0	3.7
866 399 309/35.5	311/33.6	33	2.6	3.2
848 500 431/31.5	211/34.0	35	2.5	3.2

pair quoted as Miller indices/degrees for the smallest angle of misorientation.

Column 2: axis/angle pair of the closest CSL configuration to the boundary in column 1 ($\Sigma \leqslant 49$).

Column 3: value of Σ for the CSL in column 2 and the experimental boundary in column 1.

Column 4: the maximum angular deviation from the exact CSL which can be accommodated by grain-boundary dislocations (V_m).

Column 5: the computed angular deviation of the experimental boundary (column 1) from the exact CSL (column 2) (V). It has been shown by the present authors that the computed value of V is independent of which of the 24 axis/angle pair solutions is chosen [24].

The inclusion of a group of boundaries in Table II which are designated "near CSL" needs some justification. Boundaries which are about 0.5° outside the adopted criterion for a CSL limit comprise this group. Since a variation of about 0.2° is inherent in the matrix manipulation technique which generates the smallest angle solution for a given axis/angle pair [16] some of these boundaries may well fit the CSL case as defined. Alternatively, the interpretation placed upon "near CSL" boundaries could indicate that such boundaries have been in the process of rotating towards a CSL configuration.

Boundaries are listed in order of increasing misorientation from the exact CSL case for all three heat treatments, unaged, aged and overaged. A summary of the final analysis of CSL and non-CSL boundaries is given in Table II.

4. Discussion

Table II shows a clear correlation between boundary pinning and proportion of CSL boundaries. The unpinned boundaries (unaged specimen), which have undergone considerable grain boundary migration, have a proportion of CSL boundaries which agrees fairly well with that predicted from statistical considerations [25]. Where the specimen has been aged the proportion of CSL boundaries is higher, and for the overaged specimen (where the boundaries are strongly pinned such that grain growth has been suppressed during the 1000 h heat treatment) almost half the sampled boundaries are of the CSL type. Such an increase could be the consequence of a strong texture; however, the data in Table III (obtained by the method of Horta *et al.* [26]) shows that the texture is not greatly altered. An alternative explanation will be offered which is consistent with the microstructural changes that have taken place as a consequence of strong boundary pinning.

4.1. Boundary/precipitate interactions

The inhibition of grain growth during ageing has been explained in terms of the strong pinning force exerted on grain boundaries by γ' precipitates. This has been discussed in detail elsewhere [14, 27]. Briefly, it was shown that enhanced coarsening of γ' arose from interaction with grain boundaries, concomitant with a local increase in volume fraction of the phase which effectively doubles the pinning force per unit area of boundary. The driving force for boundary migration is insufficient to overcome such a strong drag and grain growth is completely inhibited. While most of

TABLE II

Heat treatment	Number of boundaries analysed	CSL (%)	Near CSL (%)	Low angle (%)	Total non-CSL (%)
Unaged	43	18.5	9	2	82.5
Aged	74	27	8	9.5	73
Overaged	77	47	11.5	5	53

TABLE III Percentage of planes with orientation f

f	Unaged (%)	Aged (%)	Overaged (%)
111	6	6	5
200	6	4	5
220	17	15	19
311	25	22	27
331	19	21	22
420	16	31	19
422	11	2	2

the observed interactions of grain boundaries with γ' involved pinning, some cases existed where the boundary was actually cutting through a precipitate while allowing full particle/matrix coherency to be maintained [14]. Most commonly, this kind of event occurred in conjunction with a faceted boundary (Fig. 1). The interpretation of previous work to explain the occurrence of faceting does not always support the explanation that the tendency of CSL planes containing a high density of coincident sites to be incorporated in the boundary leads to the faceted boundary structure [8]. However, the occurrence of faceting through coherent, ordered γ' would tend to imply that, for these cases, the facet plane is of particularly low energy since the cutting of γ' is a difficult process kinetically [12, 14]. Fig. 2 shows a γ' precipitate has been cut by one of the boundary facets. Gamma prime precipitates which show both the typical morphology of a coherent grain-boundary precipitate and typical size relative to matrix precipitates are indicated in Fig. 1, which shows a near $\Sigma = 43$ and a $\Sigma = 31$ boundary, in a post-aged specimen.

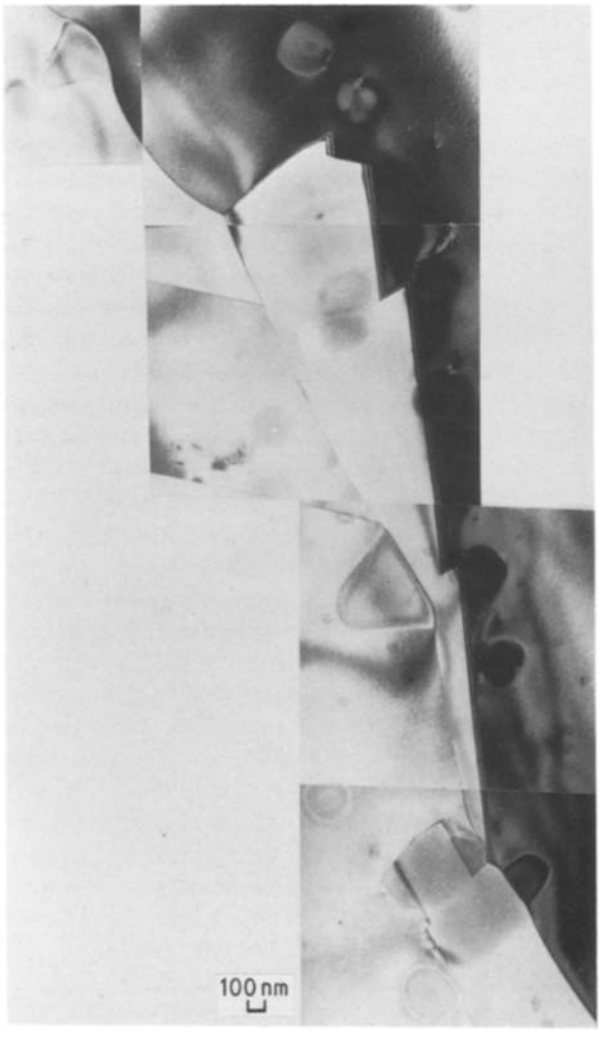

Figure 1 Montage showing the typical morphology and size of intergranular gamma-prime precipitates relative to intragranular precipitates after overageing. Both pinning and cutting interactions can be seen.

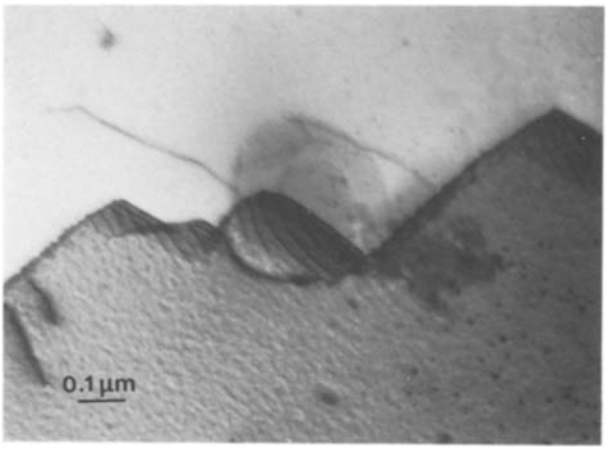

Figure 2 Part of a faceted, random boundary cutting through a γ' precipitate.

No correlation could be found between the nature of the boundary/γ' interaction with respect to density, size and morphology of the precipitates and CSL/non-CSL boundaries. This is not surprising because, although there is some evidence that nucleation frequency (and subsequently density) of precipitates can be related to boundary structure [28], the situation here is that γ' nucleates homogeneously within grains [29] and intergranularly sited precipitates are the result of subsequent pinning interactions.

4.2. Energy changes

A direct result of the inhibition of grain-boundary migration during ageing is that boundaries are prevented from lowering their energies via a reduction in grain-boundary area – the conventional driving force for grain growth. Instead of grain-boundary migration, the movement of some grains has been rotational, resulting in an increase in CSL boundaries. Since the usual translational migration events result in a reduction of energy, it is reasonable to assume that the grain rotations bring about a similar overall reduction in energy. Recent work [30] shows that during grain growth the average grain-boundary energy increases; however, the overall energy of the system is still lowered because of the net decrease in grain-boundary area. The situation discussed in the present study is a direct converse of the grain growth case because boundaries are pinned. It is reasonable then that grain-boundary energy should decrease for the pinned (constant grain-boundary area) situation since it has been shown to increase for the unpinned (reduction grain-boundary area) case. It is only possible to conduct a very approximate calculation of the energy reduction associated with the increase in CSL orientations observed for the pinned boundary regime (overaged data) because the exact energy of each boundary is not known and may vary widely with boundary-

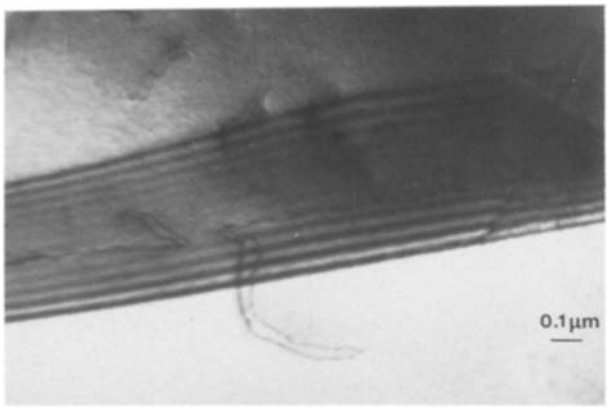

Figure 3 The incorporation of a lattice dislocation pair into a grain-boundary and subsequent dissociation along the boundary in an aged specimen.

plane inclination [19]. Other workers have assumed that the average energy of an exact CSL boundary is 15% less than for the random case [10, 11]. However, for application to this data, it is probably more realistic to assume that the energies of CSL boundaries are on average 10% less than random, as many boundaries are a few degrees away from a precise CSL orientation (Table I):

Energy of a random boundary in PE16 [31] $= 750\,\mathrm{mJ\,m^{-2}}$

Therefore, energy of a CSL boundary $= 675\,\mathrm{mJ\,m^{-2}}$

Total grain-boundary area pre-ageing $= A\,\mathrm{m^2}$ = total grain-boundary area post-ageing

Total grain-boundary energy in system pre-ageing $= 0.27 \times 675A + 0.73 \times 750A = 730A\,\mathrm{mJ\,m^{-2}}$

Total grain boundary energy in system post-ageing $= 0.47 \times 675A + 053 \times 750A = 715A\,\mathrm{mJ\,m^{-2}}$

This calculation shows that of the order of a 2% energy reduction has occurred during ageing, despite the absence of grain growth.

4.3. Mechanism of grain rotations

The results presented here suggest that grain boundaries are able to change their structures and therefore lower their energies by grain rotations which increase the degree of order at the boundary when the normal mechanism of energy reduction by grain-boundary migration is blocked. It now remains to discuss the mechanism by which such rotations are able to occur. During phenomena such as recrystallization or creep, boundary structure modifications take place by the absorption of lattice dislocations (e.g. [32]). A similar mechanism has been put forward to explain the rotation of a random boundary into a $\Sigma = 21$ type during high-temperature creep deformation [33]. The main argument against boundary absorption of lattice dislocations being the only mechanism for this situation is that the experiment was conducted using fully recrystallized specimens and therefore the density of dislocations in the lattice would be expected to be low. However, it has been shown that it is boundary, rather than lattice diffusion which is important in order that structural rearrangements at boundaries may take place [34]. The rearrangements of dislocations in the boundary will inevitably involve climb processes which are dependent upon point defect diffusion in the boundary. Athough the boundaries investigated here are stationary because of strong pinning, they are none the less under the influence of a driving force for grain-boundary migration.

The process described above is illustrated in Fig. 3 which shows the incorporation into a random boundary in an unaged specimen of a lattice dislocation pair which subsequently dissociates along the boundary. The dislocation pairing seen in Fig. 3 is a consequence of ordering of the γ' phase. Extrinsic grain-boundary dislocations are not commonly observed in random boundaries because the open structure of the random boundary allows them to dissociate, as seen in Fig. 3 [35]. The same process in an ordered (i.e. CSL) boundary is more difficult, and lattice dislocations which impinge upon such a boundary are not able to dissociate because of the smaller capacity for diffusion and climb in the more closely packed structure (e.g. [36]). It is therefore only in CSL boundaries that extrinsic grain-boundary dislocations tend to be seen. Fig. 4 shows three sets of such dislocations in a $\Sigma = 5$ boundary in an aged specimen. This extrinsic structure precludes the absorption of more lattice

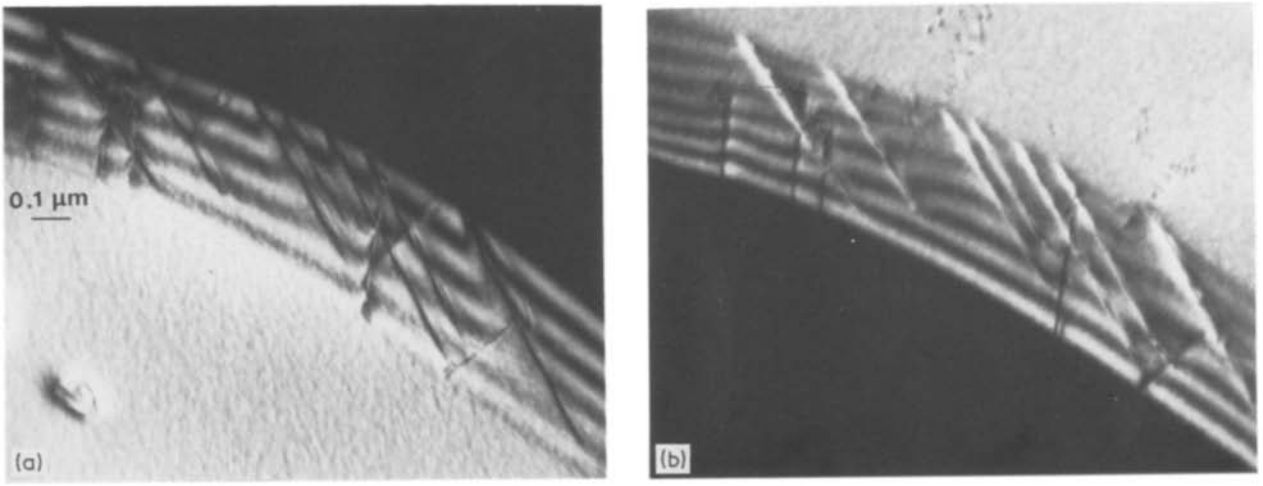

Figure 4 $\Sigma = 5$ grain-boundary with (a) upper grain and (b) lower grain in a two-beam orientation. Three sets of extrinsic grain-boundary dislocations are visible.

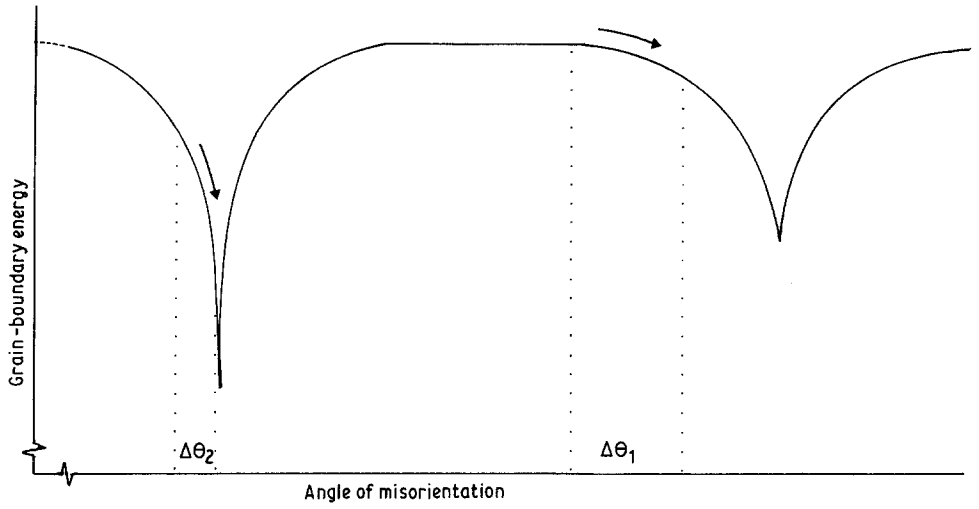

Figure 5 Schematic diagram illustrating the reduction in grain-boundary energy which would occur if the boundary were to approach an energy cusp via a rotation through $\Delta\theta_1$ or $\Delta\theta_2$.

dislocations which would further modify the boundary structure. Consequently, once a boundary has attained a "close packed" CSL structure, it will not tend to degenerate into a CSL of a lower Σ value unless there are special circumstances which favour this dissociation, such as twinning [37]. This accounts for the spread of CSL values recorded in the data.

While the differential incorporation of lattice defects into grain boundaries, as discussed above, can obviously be invoked to explain some of the reorientation of grains it is unlikely that this is the dominant mechanism. It seems more likely that the relative and cooperative sliding of grains is the main mechanism. To invoke this idea requires a cooperative sliding process with suitable adjustments at grain corners and grain edges. For boundaries which already have a periodic structure consisting of grain-boundary dislocations this merely implies the glide and climb of these in such a way as to allow the grains to slide past each other. Given the fact that it is the reduction in grain-boundary energy which drives this process it is reasonable to suggest that this sliding process would favour a situation where the net dislocation content of a boundary is reduced. For boundaries initially far removed from a CSL orientation with no periodic relaxations, the sliding process might initially be expected to be dominated by the adjustments in orientation of grain boundaries connected to it through grain edges and corners. Its sliding would then be essentially a diffusion process until its misorientation happens to approach a CSL situation. This situation is indicated by $\Delta\theta_1$ on the schematic energy/rotation angle plot in Fig. 5. At this stage it begins to assume an ordered periodic structure with arrays of grain-boundary dislocation. Subsequent sliding of a boundary which already has such a structure would then follow via a rotation through $\Delta\theta_2$, approaching the exact CSL orientation which corresponds to the energy minimum.

5. Conclusion

1. The grain-boundary geometries of three sample populations for unaged, aged and overaged heat-treatment conditions of the alloy Nimonic PE16 have been analysed.

2. While the proportion of CSL boundaries in the unaged population agree with the expected value, the aged and overaged sets show an increase in the fraction of CSL boundaries, such that half the boundaries in the over-aged sample were of this type.

3. The increase in proportion of CSL boundaries as a function of heat treatment is interpreted as a direct consequence of the pinning of grain boundaries by coherent γ' precipitates. Grain-boundary migration is prevented, so it is suggested that as an alternative means of lowering the system's energy, some grains rotate into CSL geometries, which, by implication, are energetically favourable configurations.

Acknowledgements

Financial support and permission to publish this paper from the United Kingdom Atomic Energy Authority, the Central Electricity Generating Board, and SSEB is gratefully acknowledged.

References

1. B. RALPH, R. C. ECOB, A. J. PORTER, C. Y. BARLOW and N. R. ECOB, In Proceedings of the 2nd Risø International Symposium, Denmark, 1981 (Risø National Laboratory Press, Roskilde, 1981) p. 111.
2. W. BOLLMAN, "Crystal Lattices, Interfaces and Matrices", (Imprimerie des Bergues, Geneva, 1982).
3. G. H. BISHOP and B. CHALMERS, *Scripta Met.* **2** (1971) 133.
4. T. OGURA, C. J. McMAHON, H. C. FENG and V. VITEK, *Acta Met.* **26** (1978) 1317.
5. J. D. RUSSELL and A. T. WINTER, *Scripta Met.* **19** (1985) 575.
6. H. GLEITER and B. CHALMERS, *Prog. Mater. Sci.* **16** (1972) 139.
7. G. HERRMANN, H. GLEITER and G. BARO, *Acta Met.* **24** (1976) 353.
8. P. J. GOODHEW, "Grain Boundary Structure and Kinetics" (ASM, Ohio, 1980) p. 155.
9. L. S. SHVINDLERMAN and B. B. STRAUMAL, *Acta Met.* **33** (1985) 1735.
10. R. VISWANATHAN and C. L. BAUER, *Met. Trans.* **4** (1973) 2645.

11. K. T. AUST, "Surfaces and Interfaces" Vol. I (Syracuse University Press, 1966) p. 435.
12. D. DOHERTY, *Met. Sci.* **16** (1982) 1.
13. E. GRANT, A. J. PORTER and B. RALPH, *J. Mater. Sci.* **19** (1984) 3554.
14. V. RANDLE and B. RALPH, *Acta Met.* **34** (1986) 891.
15. D. G. BRANDON, B. RALPH, S. RANGANATHAN and M. S. WALD, *ibid.* **12** (1964) 813.
16. V. RANDLE and B. RALPH, *J. Mater. Sci.* **21** (1986) 3823.
17. P. H. PUMPHREY, *Scripta Met.* **6** (1972) 107.
18. B. RALPH, P. R. HOWELL and T. F. PAGE, *Phys. Stat. Sol. B.* **55** (1973) 641.
19. H. GLEITER, *Z. Metallkde* **61** (1970) 282.
20. Y. ISHIDA and M. McLEAN, *Phil. Mag.* **27** (1973) 1125.
21. D. G. BRANDON, *Acta Met.* **14** (1966) 1479.
22. Y. ISHIDA, *Trans. Jpn. Inst. Met.* **11** (1970) 107.
23. D. H. WARRINGTON and H. GRIMMER, *Phil. Mag.* **30** (1974) 461.
24. V. RANDLE and B. RALPH, International Physics Conference Series No. 78, EMAG '85, (Adam Hilger, 1985), p. 59.
25. D. H. WARRINGTON and M. BOON, *Acta Met.* **23** (1975) 599.
26. R. M. S. B. HORTA, W. T. ROBERTS and D. V. WILSON, *Trans. AIME* **245** (1969) 2525.
27. V. RANDLE, B. RALPH and N. HANSEN, 7th Risø International Symposium, Denmark, 1986, p. 123.
28. P. N. T. UNWIN and R. B. NICHOLSON, *Acta Met.* **17** (1969) 1379.
29. E. NEMBACH and G. NEITE, *Prog. Mater. Sci.* **29** (1985) 177.
30. W. PRZETAKIEWICZ, K. J. KURZYDLOWSKI and M. W. GRABSKI, *Mater. Sci. Tech.* Feb (1986) 106.
31. L. E. MURR, "Interfacial Phenomena in Metals and Alloys" (Addison-Wesley, 1975).
32. A. R. JONES, P. R. HOWELL and B. RALPH, *Phil. Mag.* **35** (1977) 603.
33. H. KOKAWA, T. WATANABE and S. KARASHIMA, *Scripta Met.* **17** (1983) 1155.
34. P. H. PUMPHREY and H. GLEITER, *Phil. Mag.* **30** (1974) 32.
35. H. KOKAWA, T. WATANABE and S. KARASHIMA, *ibid.* **44A** (1981) 1239.
36. A. H. KING, *Scripta Met.* **19** (1985) 1517.
37. P. J. GOODHEW, *Met. Sci.* **13** (1979) 108.

Received 26 August
and accepted 9 October 1986